NMRlipids IV: Headgroup & glycerol backbone structures, and cation binding in bilayers with PE and PG lipids

Amélie Bacle,[1] Pavel Buslaev,[2] Rebeca García Fandiño,[3,4] Fernando Favela-Rosales,[5] Tiago Ferreira,[6] Patrick Fuchs,[1] Matti Javanainen,[7] Anne M. Kiirikki,[8] Jesper J. Madsen,[9,10] Josef Melcr,[7,11] Paula Milan Rodriguez,[1] Markus S. Miettinen,[12] O. H. Samuli Ollila,[8,*] Chris G. Papadopoulos,[13] Antonio Peón,[14] Thomas J. Piggot,[15] and Ángel Piñeiro[16]

[1]*Paris, France*
[2]*University of Jyväskylä*
[3]*Center for Research in Biological Chemistry and Molecular Materials (CiQUS), Universidade de Santiago de Compostela, E-15782 Santiago de Compostela, Spain*
[4]*CIQUP, Centro de Investigao em Qumica, Departamento de Qumica e Bioqumica, Faculdade de Citncias, Universidade do Porto, Porto, Portugal*
[5]*Departamento de Investigación, Tecnológico Nacional de México, Campus Zacatecas Occidente, México*
[6]*Halle, Germany*
[7]*Institute of Organic Chemistry and Biochemistry of the Czech Academy of Sciences, Flemingovo nám. 542/2, CZ-16610 Prague 6, Czech Republic*
[8]*Institute of Biotechnology, University of Helsinki*
[9]*Department of Chemistry, The University of Chicago, Chicago, Illinois, United States of America*
[10]*Department of Global Health, College of Public Health, University of South Florida, Tampa, Florida, United States of America*
[11]*Groningen Biomolecular Sciences and Biotechnology Institute and The Zernike Institute for Advanced Materials, University of Groningen, 9747 AG Groningen, The Netherlands*
[12]*Department of Theory and Bio-Systems, Max Planck Institute of Colloids and Interfaces, 14424 Potsdam, Germany*
[13]*I2BC - University Paris Sud*
[14]*Spain*
[15]*Chemistry, University of Southampton, Highfield, Southampton SO17 1BJ, United Kingdom*
[16]*Departamento de Física Aplicada, Facultade de Física, Universidade de Santiago de Compostela, E-15782 Santiago de Compostela, Spain*

(Dated: January 12, 2021)

Chemistry of lipid headgroups, the water facing components of cell membranes that regulate cell functions via lipid–protein interactions, varies between organisms and organelles. Because lipid membranes are in liquid state under physiological conditions, the conformational ensembles of lipid headgroups and their dependence on chemistry are difficult to resolve experimentally. Here, we combine solid state NMR experiments and molecular dynamics simulations from NMRlipids open collaboration to resolve the conformational ensembles of the headgroups of key lipid types in liquid lamellar phase under various biologically relevant conditions. Interpretation of NMR experiments using the plethora of simulation data collected in the NMRlipids project suggests that all lipid headgroups sample a wide range of conformations in neutral and charged cellular membranes. However, the populations of different conformations are dictated by the headgroup chemistry. Together with the analysis of protein-bound lipids from the protein data bank (PDB), this suggests that lipids can bind to proteins in wide range of conformations independently on the headgroup chemistry. Therefore, the selective adsorption of proteins to membranes is likely regulated by specific protein–lipid interactions, rather than conformational restrictions of lipids. Our results pave the way to comprehensive understanding of lipid–protein interaction energetics, and the understanding of complex biomolecular assemblies such as membrane proteins.

INTRODUCTION

Chemical compositions of hydrophilic lipid headgroups vary between different organelles and organisms, and different lipid types regulate protein functions in many different ways [1, 2]. Lipids can directly bind to proteins or indirectly affect protein functions by altering membrane properties or charge [1, 3]. While the specific interactions with certain lipid headgroups are known to be essential for the function of several proteins [3, 4], it is not clear if the specificity is driven by the differences in accessible conformational states between lipid types or by specific intermolecular lipid–protein interactions.

The conformational ensembles of lipids in the physiologically relevant lamellar liquid phase are typically derived from NMR experiments, particularly from C–H bond order parameters measured using ^{2}H NMR [5–7]. Notably, such measurements can be performed also on living cells [8–10]. These studies suggest that the glycerol backbone conformations are largely similar irrespectively of the headgroup [8], and the headgroup conformations are similar in PC, PE and PG lipids, while the headgroup is more rigid in PS lipids [11, 12]. However, these tendencies are based only on the absolute values, whereas the necessity of order parameter signs in capturing the conformational ensembles of lipids has been recently demonstrated [13–15]. Furthermore, the detailed understanding of lipid conformational ensembles is limited by the lack of universal models that would map order parameters to structural ensembles / that would help interpret the experiments [16, 17].

Stuctures of different lipid types in protein bound states can be extracted from the protein data bank (PDB) [18], but their relation to the conformational ensembles in liquid lamellar state remains unclear [19]. In addition to the changes in lipid conformational ensembles upon binding to proteins, also the experimentally measured response of lipid headgroup to membrane bound charges remains poorly understood due to the lack of suitable models to interpret the lipid conformational ensembles in liquid lamellar state [7].

Here, we use natural abundance ^{13}C NMR experiments and MD simulations from the NMRlipids open collaboration to resolve the differences in conformational ensembles between PC, PE, PG and PS lipid headgroups. Zwitterionic PC and PE are the most common lipids in eukaryotes and bacteria, respectively [2, 20]. PE is also the second most abundant glycerophospholipid in eukaryotic cells and has been related to various diseases [21–23]. PS and PG are the most common negatively charged lipids in eukaryotes and bacteria, respectively, and affect membrane protein functionality and signaling [3, 20, 24, 25]. All the studied lipids specifically bind to various proteins [26]. Furthermore, we use our results to elucidate lipid-protein interactions and the effect of charges on lipid conformations.

The lipid conformational ensembles in liquid lamellar state paves the way toward understanding the specific binding of different lipid types to membrane proteins and how they regulate the protein function. Because glycerol backbone and headgroup structures of PC lipids are similar in model membranes and in bacteria [8–10], the results from model systems could be used to understand the biological role of lipid headgroup conformational ensembles in different lipid types.

METHODS

Experimental C–H bond order parameters

The headgroup and glycerol backbone C–H bond order parameters of POPE and POPG were measured using natural abundance ^{13}C solid state NMR spectroscopy as described previously [15, 27]. The magnitudes of order parameters were determined from the chemical-shift resolved dipolar splittings using a R-type Proton Detected Local Field (R-PDLF) experiment [28] and the signs from S-DROSS experiments [29] combined with SIMPSON simulations [30]. The NMR experiments were identical as in our previous work [31]. POPE and POPG powder were purchased from Avanti polar lipids **1.POPG is racemic in experiments. How much we should discuss this in relation with simulations?**. The POPE experiments were recorded at 310 K and POPG experiments at 298 K, where the bilayers are in the liquid disordered phase [32].

Glycerol backbone peaks from both lipids, and α-carbon peak from POPE in the INEPT spectra were assigned based on previously measured POPC spectra [27]. The β-carbon peak from POPE was assigned based on ^{13}C chemical shift table for amines available at `https://www.chem.wisc.edu/areas/reich/nmr/c13-data/cdata.htm`. **2.How were α and γ-carbon peaks assigned in POPG?**. The β-carbon peak from POPG overlapped with the g_2 peak from glycerol backbone because their chemical environments are similar. **3.Details to be checked by Tiago**.

Molecular dynamics simulations

Molecular dynamics simulation data were collected using the NMRlipids Open Collaboration [13], which is running at `nmrlipids.blogspot.fi` and `github.com/NMRlipids/NMRlipidsIVotherHGs`. The simulated systems of pure PE and PG bilayers without additional ions are listed in Tables S1 and S2, and lipid mixtures with additional ions in Tables S3 and S4. Further simulation details are given in the SI, and the simulation data are indexed in a searchable database available at `www.nmrlipids.fi`, and in the NMRlipids/MATCH repository (`github.com/NMRlipids/MATCH`).

Analysis of molecular dynamics simulation data

The large set of MD simulation data was analysed using the development version of NMRlipids databank. Unique naming convention for lipid atoms in each force field was defined using the mapping files and analysis for all simulations indexed in NMRlipids databank manner were performed using python codes.

The C–H bond order parameters were calculated directly from the carbon and hydrogen positions using the definition

$$S_{\mathrm{CH}} = \frac{1}{2}\langle 3\cos^2\theta - 1\rangle, \qquad (1)$$

where θ is the angle between the C–H bond and the membrane normal (taken to align with z, with bilayer periodicity in the xy-plane). Angular brackets denote average over all sampled configurations. The order parameters were first calculated averaging over time separately for each lipid in the system. The average and the standard error of the mean were then calculated over different lipids. Python programs that use the MDAnalysis library [33, 34] used for all atom simulations is available in Ref. 35 (`scripts/calcOrderParameters.py`). For united atom simulations, the trajectories with hydrogens having ideal geometry were constructed first using either buildH program [36] or (`scratch/opAAUA_prod.py`) in Ref. 35, and the order parameters were then calculated from these trajectories. This approach has been tested against trajectories with explicit hydrogens and the deviations in order parameters are small [36, 37].

The ion number density profiles were calculated using the `gmx density` tool of the Gromacs sofware package [38].

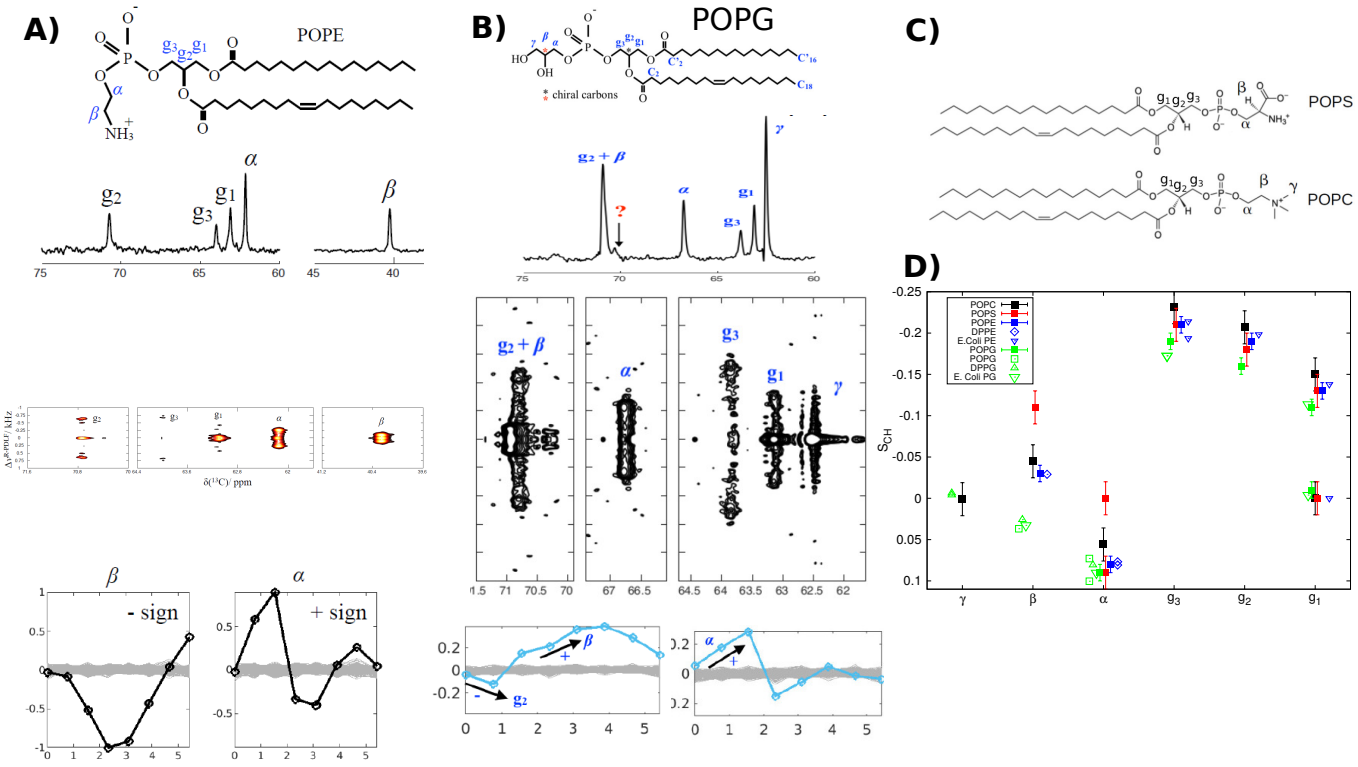

FIG. 1: Chemical structure, refocused-INEPT spectrum, 2D R-PDLF spectra, and S-DROSS data (from top to bottom) of **A)** POPE and **B)** POPG. Full NMR spectra are shown Figs. S1 and S2. **C)** Chemical structure of POPC and POPS. **D)** Headgroup and glycerol backbone order parameters from different experiments in lamellar liquid disordered phase. The values and signs for POPE (310 K) and POPG (298 K) measured in this work, and for POPS (298 K) [31] and POPC (300 K) [15, 27] previously using ^{13}C NMR. The literature values for DOPS with 0.1M of NaCl (303 K) [39], POPG with 10nM PIPES (298 K) [40], DPPG with 10mM PIPES and 100mM NaCl (314 K) [11], DPPE (341 K) [41], E.coliPE and E.coliPG (310 K) [8] are measured using ^{2}H NMR. The signs from ^{13}C NMR are used also for the literature values.

4.This is a sketch, Tiago Ferreira will make a new figure.

Analysis of lipid conformations bound to proteins

Lipid structures from PDB (`http://www.rcsb.org/`) were searched using PDBe REST API (`www.ebi.ac.uk/pdbe/pdbe-rest-api`). First, all PDB entries containing PC, PE, PG, or PS lipid headgroups were searched. The ligand names to identify the lipids were: PLC, PX4, 6PL, LIO, HGX, PC7, PC8, P1O, 6O8, XP5, EGY, PLD, SBM, HXG, and PCW for PC; 8PE, PTY, 3PE, PEH, PEF, 6OE, 6O9, 9PE, PEV, 46E, SBJ, L9Q, PEK, EPH, ZPE, 9TL, 9Y0, 6OU, LOP, and PEE for PE; PGT, PGK, LHG, 44G, PGV, OZ2, D3D, PGW, DR9, P6L, PG8, H3T, and GOT for PG; and PSF, PS6, Q3G, P5S, D39, PS2, 17F, and 8SP for PS. All PDB structures containing these ligands were downloaded and the dihedral angles of the first lipid in the latest version of the structures within each PDB code were calculated using the MDTraj python library [42]. The used Jupyter notebook is available from the project's GitHub repository (*scripts/pdbSEARCH.ipynb*).

RESULTS AND DISCUSSION

Differences between lipid headgroups in bulk bilayer from ^{13}C NMR experiments

To experimentally characterize the headgroup conformational ensembles of lipids that are not bound to proteins in electrostatically neutral cell membrane, we measured the C-H bond order parameters and their signs from of POPG and POPE in liquid lamellar phase, as we did previously for POPC and POPS [15, 27, 31]. Determination of headgroup and glycerol backbone order parameters and their signs was straightforward from the data in Figs. 1, S1 and S2 for all the C-H bonds, except the β and g_2 carbons in POPG. These carbons have overlapping peaks in the INEPT spectra due to their similar chemical environments, and only the magnitude of the larger order parameter could be determined from the R-PDLF spectra (Fig. 1 B). Nevertheless, based on previous ^{2}H NMR measurements [8, 11, 40], we assigned the larger order parameter to the g_2 carbon and used the literature value for the β-carbon in SIMPSON simulations to determine the signs. The decrease in the beginning of the S-DROSS curve suggests that the sign of larger g_2 order parameter is negative and later in-

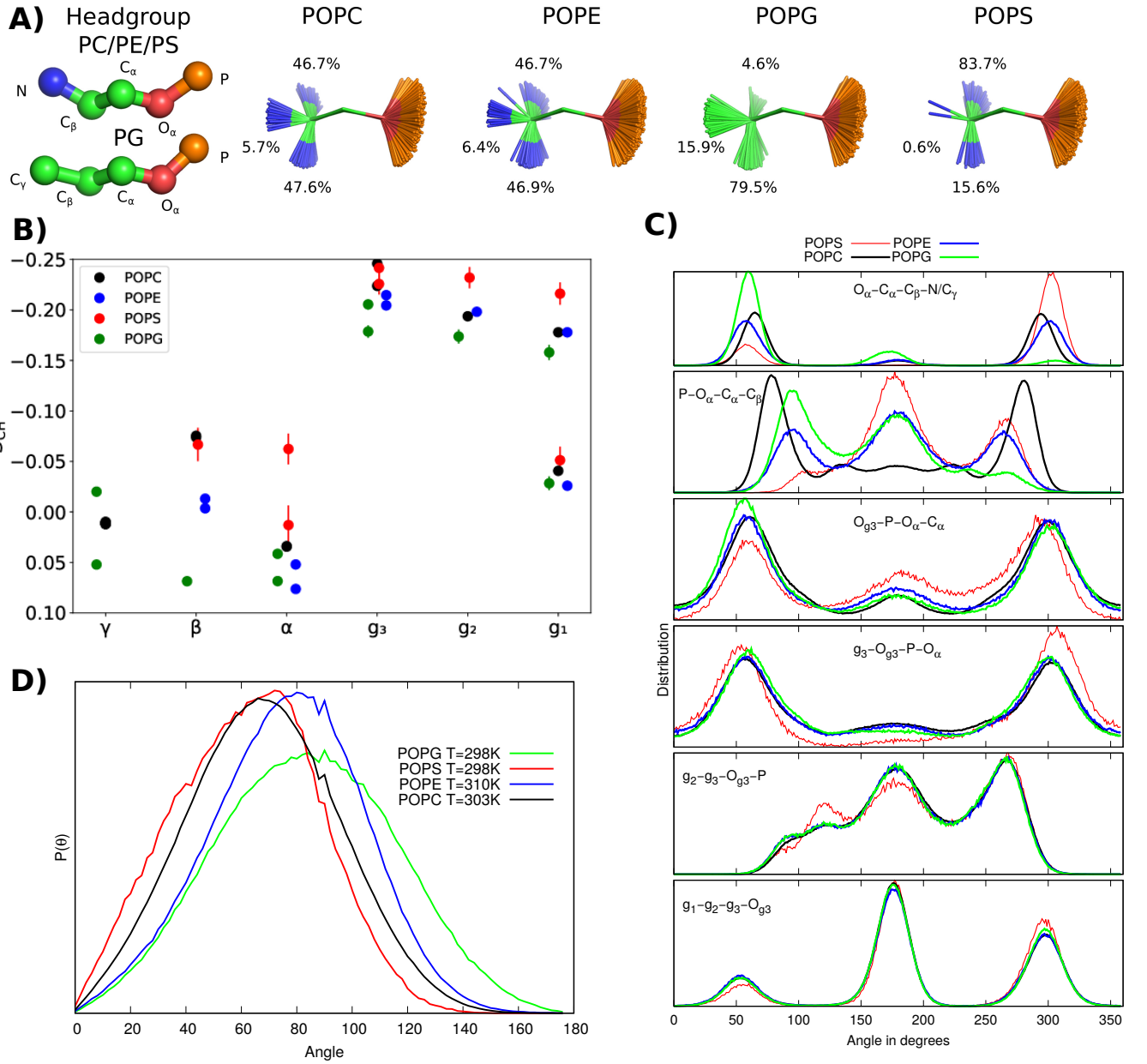

FIG. 2: Results from CHARMM36 simulations demonstrating the differences in conformational ensembles betwee different lipids. **A)** Snapshots with overlayed C_β, C_α and O_α atoms and occurence of different conformations. **B)** Headgroup and glycerol backbone region order parameters of different different lipids. **C)** Distributions of heavy atom dihedral angles of different lipids from CHARMM36 simulations. **D)** Distributions of P-N vector angle with respect to membrane normal.

5.This is a draft and requires quite a bit of polishing. More detailed discussion of this figure is in https://github.com/NMRLipids/NMRlipidsIVPEandPG/issues/9

crease suggests that sign of smaller β order parameter is positive (Fig. 1 (B)). This interpretation is confirmed by SIMPSON calculations in Fig S3.

Experimental order parameters of POPC, POPE, POPG and POPS glycerol backbones and headgroups from this and previous studies are collected in Fig. 1 D), where signs determined from ^{13}C NMR experiments are used also for the ^{2}H NMR data from the literature. Overall agreement of order parameters determined by different authors and different techniques for same lipid headgroup is very good in here and previous studies [13, 14, 31], suggesting that the observed differences between lipid types arise from differences in headgroup chemistry rather than inaccuracies in experiments, or differences in acyl or experimental conditions. The most distinct order parameters are observed for PS headgroups, for which the α-carbon order parameter exhibits significant forking and the β-carbon has more negative value than in other lipids. On the other hand, the β-carbon order parameter of PG headgroup has positive sign in contrast to all the other lipids. Notably, this has not been observed in traditional ^{2}H

NMR experiments, where only the absolute value of the order parameters are measured [8, 11, 40]. The glycerol backbone order parameters are similar for all the lipids, although they move slightly toward positive values (closer to zero) in the order PC $<$ PE $<$ PS $<$ PG. Essential differences between PC and PE headgroups are not observed.

Conformational ensembles of different lipid headgroups in bulk bilayer from MD simulations

To resolve the conformational ensembles of lipid headgroups, we compared the headgroup and glycerol backbone C-H bond order parameters from different MD simulation force fields to the experimental data. None of the force fields reproduced the order parameters within experimental accuracy for any of the lipids analysed in this work (Figs. S4 and S5) or in our previous studies [13, 31]. Nevertheless, the CHARMM36 force field performs best for all the headgroups and reproduces the experimentally observed distinct order parameters of PS and PG lipids (Fig. 2 B). To understand the structural origin of these distinct order parameters, we calculated the distributions of heavy atom dihedral angles from CHARMM36 simulations in figure 2 C). Major differences between headgroups are observed only for the last two dihedrals in the headgroup end, O_α-C_α-C_β-N/C_γ and P-O_α-C_α-C_β, which prefer *gauche*$^-$ conformations for PG and *gauche*$^+$ for PS. Rest of the dihedrals are similar between different lipids, with the exception of small differences for PS lipids. Therefore we suggest that the main differences between lipid headgroups leading to distinct order parameter occur in the choline part, while also changes in phosphate region may contribute in PS lipids, which could also explain the more rigid headgroup structures [12, 39]. Furthermore, the angle between headgroup dipole and membrane normal decreases in the order of PG $>$ PE $>$ PC $>$ PS (Fig. 2 B)). However, the differences between PC and PE in P-O_α-C_α-C_β dihedral and P-N vector dipole may be artificial as the β-carbon order parameter in PC is too negative in the CHARMM36 force field, thereby not being equal to the order parameter in PE as observed in experiments [13].

In conclusion, all lipid headgroups sample very broad conformational ensembles in liquid lamellar phase. between headgroups, the sampled dihedral angles are within approximately same ranges for all headgroup types. Therefore, we suggest that all lipid headgroups are very flexible thereby being able to adopt wide range of multiple conformations when interacting with proteins, ions or other biomolecules. Our results support the models that propose free rotation around phosphate group for PC lipids, which decouples the dynamics and conformatios between acyl chains and headgroups [44, 45], and suggests that these models could be applied for all lipids containing the phosphorus group. The wide range of observed conformations suggest that the structures in lipid crystals [12, 46] play only a minor role, and that the models aiming to explain NMR data using only few conformations [5–7, 17] are not sufficient to capture the large conformational space of lipids in liquid lamellar state.

Lipid conformational ensembles in lipid bilayers with bound ions

Charged lipids, proteins, surfactants, drugs, and ions incorporated in membranes reorient the headgroup dipole in PC lipids, thereby affecting the order parameters of lipid headgroups [47]. However, detailed understanding on lipid conformational ensembles in membranes bearing electric charge is still lacking [7].

To resolve lipid headgroup conformational ensembles in cell membrane bearing positive charge, we first analyzed CHARMM36 simulations which correctly captures the experimentally measured decrease in PC headgroup order parameters upon addition of cationic surfactants into a bilayer in figure 3 A). Heavy atom dihedral angle distributions in figure 3 B reveal that the decrease of trans state probabilities in g_2-g_3-O_{g_3}-P and g_3-O_{g_3}-P-O_α dihedrals are the major effects of positive charge on lipid headgroup conformations. Choline region remains essentially unchanged and only minor changes are observed in other dihedrals even thought almost half of the molecules in membranes are cationic surfactants. We also tried to resolve PC lipid headgroup conformational ensembles in mixed membrane with negatively charged lipids [9], but the accuracy of currently available force fields was not sufficient for this (Fig. S6).

Also binding of ions may affect the lipid headgroup conformational ensembles in physiological conditions. In line with the results from cationic surfactants, the decreased probability for the trans state of g_3-O_{g3}-P-O_α dihedral is the main structural consequence of bound ion to PC headgroup (Fig. S12 and S13) in Lipid17ecc (having the most realistic response of PC lipid headgroup order parameters to the calcium binding in Fig. S8) and CHARMM36 simulations. Response of charged lipids to the ion binding is less well understood and more difficult to capture in MD simulations [31, 52]. The most realistic simulations (Lipid17 and Slipids in figure S8) suggest that the upward tilting of the headgroup dipole upon addition of $CaCl_2$ is weaker in PG than in PC headgroup, but dihedral distributions are more sensitive to the bound ions in PG (Figs S14 and S15). However, the changes in dihedrals upon addition of calcium differ between the best models (Figs S14 and S15), none of the simulations captures the calcium binding affinity and conformational ensemble of PG lipids simultaneously, and experimental data to evaluate the response of α-carbon order parameters to the added calcium in PG is not available. Therefore, more accurate force fields are required for the detailed analysis of the interactions between ions and charged lipids, as concluded previously also for PS lipids [31, 52].

Despite the limited capability of simulations to interpret some of the experimental data due to the inaccuries in force fields, we conclude that the experimentally observed changes in headgroup order parameters upon addition of charges into

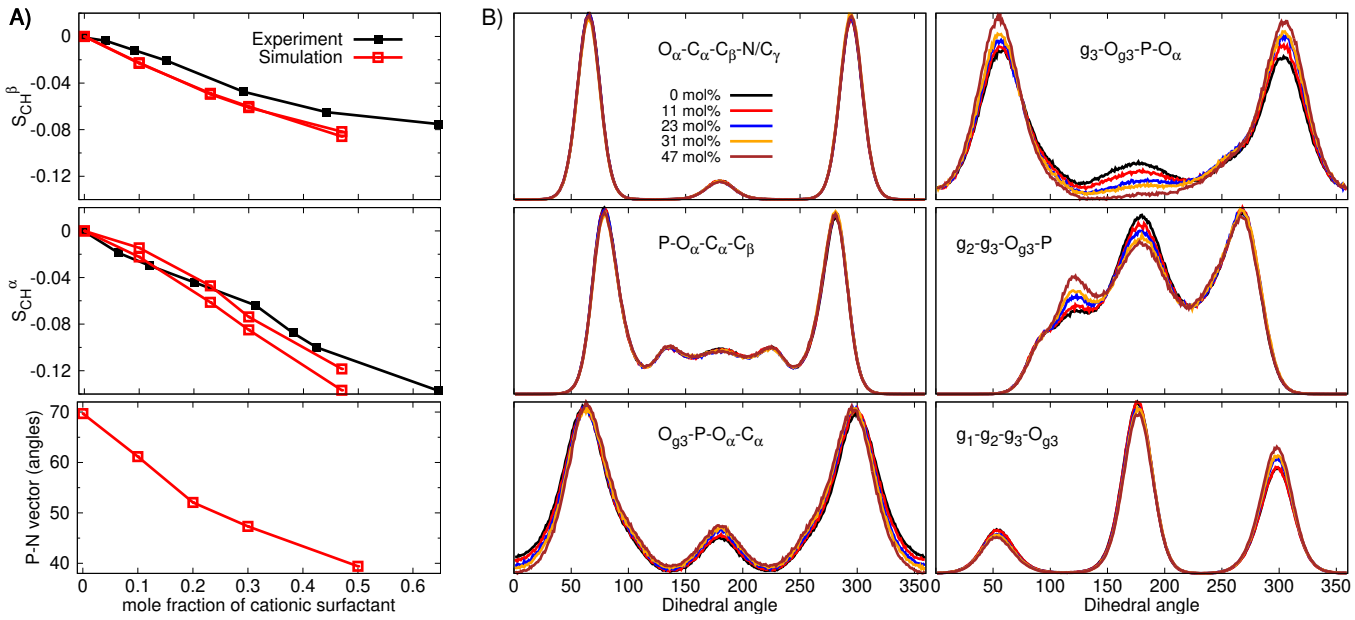

FIG. 3: **A)** Modulation of PC headgroup order parameters and P-N vector angle upon addition of cationic surfactant from CHARMM36 simulations compared with the experimental data [43]. **B)** Changes in PC headgroup conformational ensembles upon increasing the amount of positive charge in bilayer, characterized by the heavy atom dihedral distributions, from CHARMM36 simulations.

bilayer arise from relatively small changes in conformational ensembles. These changes eventuate from mild changes in dihedral angle distributions, rather than from restriction of lipids into fixed conformations. Therefore, lipid headgroups remain in disordered state sampling large space of different conformations, thereby being able to interact with different molecules in various ways, also in membranes bearing electric charge.

Protein bound lipid conformations

To analyze lipid conformations in protein bound states, we calculated the heavy atom dihedral distributions from all lipid conformations available within protein structures deposited in the PDB [18] in figure 4. We found 176 PC, 198 PE, 70 PG, and 41 PS conformations, which present lipids that are tightly bound to proteins in fixed conformations that can be determined as a part of protein structure using crystallography, NMR, or cryo-EM.

Similarly to the liquid lamellar state, lipid dihedrals have very wide range of angles when bound to proteins. Only P-O_α-C_α-C_β and g_2-g_3-O_{g_3}-P dihedrals seem to avoid cis conformations as observed also in liquid lamellar state. The O_α-C_α-C_β-N/C_γ and g_1-g_2-g_3-O_{g_3} dihedrals are even less restricted in protein bound state than in liquid lamellar phase where cis and anti ecplipsed state were not present (Fig. 2). Major differences between different lipid headgroups are not observed when bound to proteins. Slight preference for the trans state in O_α-C_α-C_β-/C_γ dihedral of PC, and for positive angles in P-O_α-C_α-C_γ dihedral of PS lipids with respect to other lipids could be present in the data, but the statistics is not sufficient for conclusions. Therefore, the differences in conformational ensembles between different lipids in liquid lamellar state in Fig. 2 are not seen in the protein bound states.

This suggests that lipids can bind to proteins in wide range of conformations independently of headgroup chemistry. Thereby, lipids compromize their preferred conformations when binding to proteins and the binding of lipids to specific locations would be driven by the intermolecular interactions between proteins and lipids. However, it is important to note that lipids are often not the main target in structures deposited in PDB and therefore their conformations may be less reliable than proteins. Stereochemical violations and structures deviating from lipid crystals have been previously proposed to indicate inaccuracies in lipid structures in PDB [16, 19]. However, we see large deviations from lipid crystals structures also in conformational ensembles that reproduce the NMR data in liquid lamellar phase, thereby proposing that such deviations are realistic also in protein bound states.

CONCLUSIONS

Conformational ensembles resolved using solid state NMR experiments and MD simulations from NMRlipids open collaboration revealed that headgroups of the most abundant biological phopholipids, PC, PE, PG and PS, sample wide range of different conformations in lamellar liquid state. Differences in NMR order parameters between different headgroups can be explained by the changes in dihedral angle distributions, suggesting that similar conformations are accessed by all

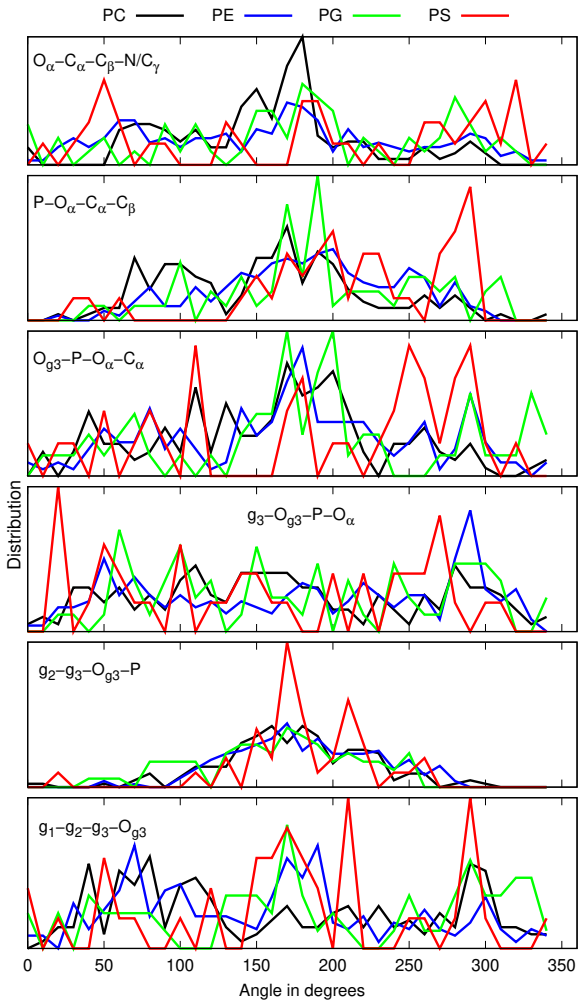

FIG. 4: Dihedral distributions from simulations and lipid structures in PDB.

headgroups, but with different probabilities. Also the changes in order parameters upon addition of charged molecules, such as cationic lipids, surfactants, or drugs, in membranes can be explained by the changes in dihedral angle probabilities, particularly close to the phosphate region.

Wide range of conformations are observed also in lipids that are tightly bound to proteins in PDB, suggesting that the specific binding of lipids to proteins is dominated by the intermolecular lipid-protein interactions, while the differences in conformational ensembles between different lipid types play a minor role. Therefore, lipids can conform themself to multiple binding positions locating in various proteins.

Our results pave the way to understand how lipids regulate membrane protein function. Lipid conformational ensembles in liquid lamellar phase are necessary for the detailed analysis of lipid-protein interaction energetics, particularly for the entropic part. Furthermore, our results demonstrate how the NMRlipids databank, containing MD simulations and NMR data, can be used to resolve conformational ensembles of disordered biomolecules in membrane environment, and how this information can be coupled with structural data in the PDB. We believe that this combination brings us closer to the comprehensive understanding of complex biomolecular assemblies containg both disordered and structural regions, such as membrane protein complexes.

AP is grateful to the Centro de Supercomputacin de Galicia (CESGA) for use of the Finis Terrae computer

* samuli.ollila@helsinki.fi

[1] A. Lee, Biochimica et Biophysica Acta (BBA) - Biomembranes **1612**, 1 (2003), ISSN 0005-2736, URL http://www.sciencedirect.com/science/article/pii/S0005273603000567.

[2] G. van Meer, D. R. Voelker, and G. W. Feigenson, Nature Reviews Molecular Cell Biology **9**, 112 (2008), URL https://doi.org/10.1038/nrm2330.

[3] M. A. Lemmon, Nat. Rev. Mol. Cell Biol. **9**, 99 (2008).

[4] A. G. Lee, Trends in Biochemical Sciences **36**, 493 (2011), URL https://doi.org/10.1016/j.tibs.2011.06.007.

[5] J. Seelig, Q. Rev. Biophys. **10**, 353 (1977).

[6] J. H. Davis, Biochim. Biophys. Acta **737**, 117 (1983).

[7] D. J. Semchyschyn and P. M. Macdonald, Magn. Res. Chem. **42**, 89 (2004).

[8] H. U. Gally, G. Pluschke, P. Overath, and J. Seelig, Biochemistry **20**, 1826 (1981).

[9] P. Scherer and J. Seelig, EMBO J. **6** (1987).

[10] J. Seelig, Cell Biology International Reports **14**, 353 (1990), ISSN 0309-1651, URL http://www.sciencedirect.com/science/article/pii/030916519091204H.

[11] R. Wohlgemuth, N. Waespe-Sarcevic, and J. Seelig, Biochemistry **19**, 3315 (1980).

[12] G. Büldt and R. Wohlgemuth, The Journal of Membrane Biology **58**, 81 (1981), ISSN 1432-1424, URL http://dx.doi.org/10.1007/BF01870972.

[13] A. Botan, F. Favela-Rosales, P. F. J. Fuchs, M. Javanainen, M. Kanduč, W. Kulig, A. Lamberg, C. Loison, A. Lyubartsev, M. S. Miettinen, et al., J. Phys. Chem. B **119**, 15075 (2015).

[14] O. S. Ollila and G. Pabst, Biochimica et Biophysica Acta (BBA) - Biomembranes **1858**, 2512 (2016).

[15] T. M. Ferreira, R. Sood, R. Bärenwald, G. Carlström, D. Topgaard, K. Saalwächter, P. K. J. Kinnunen, and O. H. S. Ollila, Langmuir **32**, 6524 (2016).

[16] W. Pezeshkian, H. Khandelia, and D. Marsh, Biophysical Journal **114**, 1895 (2018), ISSN 0006-3495, URL http://www.sciencedirect.com/science/article/pii/S0006349518302467.

[17] H. Akutsu, Biochimica et Biophysica Acta (BBA) - Biomembranes **1862**, 183352 (2020), URL https://doi.org/10.1016/j.bbamem.2020.183352.

[18] H. M. Berman, J. Westbrook, Z. Feng, G. Gilliland, T. N. Bhat, H. Weissig, I. N. Shindyalov, and P. E. Bourne, Nucleic Acids Research **28**, 235 (2000), ISSN 0305-1048, https://academic.oup.com/nar/article-pdf/28/1/235/9895144/280235.pdf, URL https://doi.org/10.1093/nar/28.1.235.

[19] D. Marsh and T. Páli, European Biophysics Journal **42**, 119 (2013), URL https://doi.org/10.1007/s00249-012-0816-6.

[20] C. Sohlenkamp and O. Geiger, FEMS Microbiology Reviews **40**, 133 (2015).

[21] J. E. Vance, Traffic **16**, 1 (2015).

[22] E. Calzada, O. Onguka, and S. M. Claypool (Academic Press, 2016), vol. 321 of *International Review of Cell and Molecular Biology*, pp. 29 – 88.

[23] D. Patel and S. N. Witt, Oxidative Medicine and Cellular Longevity **2017**, 4829180 (2017).

[24] P. A. Leventis and S. Grinstein, Annual Review of Biophysics **39**, 407 (2010).

[25] P. Hariharan, E. Tikhonova, J. Medeiros-Silva, A. Jeucken, M. V. Bogdanov, W. Dowhan, J. F. Brouwers, M. Weingarth, and L. Guan, BMC Biology **16**, 85 (2018).

[26] P. L. Yeagle, Biochimica et Biophysica Acta (BBA) - Biomembranes **1838**, 1548 (2014), membrane Structure and Function: Relevance in the Cell's Physiology, Pathology and Therapy.

[27] T. M. Ferreira, F. Coreta-Gomes, O. H. S. Ollila, M. J. Moreno, W. L. C. Vaz, and D. Topgaard, Phys. Chem. Chem. Phys. **15**, 1976 (2013).

[28] S. V. Dvinskikh, H. Zimmermann, A. Maliniak, and D. Sandstrom, J. Magn. Reson. **168**, 194 (2004).

[29] J. D. Gross, D. E. Warschawski, and R. G. Griffin, J. Am. Chem. Soc. **119**, 796 (1997).

[30] M. Bak, J. T. Rasmussen, and N. C. Nielsen, Journal of Magnetic Resonance **147**, 296 (2000), ISSN 1090-7807, URL `http://www.sciencedirect.com/science/article/pii/S1090780700921797`.

[31] H. S. Antila, P. Buslaev, F. Favela-Rosales, T. Mendes Ferreira, I. Gushchin, M. Javanainen, B. Kav, J. J. Madsen, J. Melcr, M. S. Miettinen, et al., The Journal of Physical Chemistry B p. acs.jpcb.9b06091 (2019), ISSN 1520-6106.

[32] D. Marsh, *Handbook of Lipid Bilayers, Second Edition* (RSC press, 2013).

[33] N. Michaud-Agrawal, E. J. Denning, T. B. Woolf, and O. Beckstein, Journal of Computational Chemistry **32**, 2319 (2011), https://onlinelibrary.wiley.com/doi/pdf/10.1002/jcc.21787, URL `https://onlinelibrary.wiley.com/doi/abs/10.1002/jcc.21787`.

[34] Richard J. Gowers, Max Linke, Jonathan Barnoud, Tyler J. E. Reddy, Manuel N. Melo, Sean L. Seyler, Jan Domaski, David L. Dotson, Sbastien Buchoux, Ian M. Kenney, et al., in *Proceedings of the 15th Python in Science Conference*, edited by Sebastian Benthall and Scott Rostrup (2016), pp. 98 – 105.

[35] ohsOllila and et al., *Match github repository*, URL `https://github.com/NMRLipids/MATCH`.

[36] P. Fuchs and et al., *Buildh github repository*, URL `https://github.com/patrickfuchs/buildH`.

[37] T. J. Piggot, J. R. Allison, R. B. Sessions, and J. W. Essex, J. Chem. Theory Comput. **13**, 5683 (2017).

[38] M. Abraham, D. van der Spoel, E. Lindahl, B. Hess, and the GROMACS development team, *GROMACS user manual version 5.0.7* (2015), URL `www.gromacs.org`.

[39] J. L. Browning and J. Seelig, Biochemistry **19**, 1262 (1980).

[40] F. Borle and J. Seelig, Chemistry and Physics of Lipids **36**, 263 (1985).

[41] J. Seelig and H. U. Gally, Biochemistry **15**, 5199 (1976).

[42] R. T. McGibbon, K. A. Beauchamp, M. P. Harrigan, C. Klein, J. M. Swails, C. X. Hernández, C. R. Schwantes, L.-P. Wang, T. J. Lane, and V. S. Pande, Biophysical Journal **109**, 1528 (2015).

[43] P. G. Scherer and J. Seelig, Biochemistry **28**, 7720 (1989).

[44] J. B. Klauda, M. F. Roberts, A. G. Redfield, B. R. Brooks, and R. W. Pastor, Biophys. J. **94**, 3074 (2008).

[45] H. S. Antila, A. Wurl, O. H. S. Ollila, M. S. Miettinen, and T. M. Ferreira, *Quasi-uncoupled rotational diffusion of phospholipid headgroups from the main molecular frame* (2020), 2009.06774.

[46] I. Pascher, M. Lundmark, P.-G. Nyholm, and S. Sundell, Biochim. Biophys. Acta **1113**, 339 (1992).

[47] J. Seelig, P. M. MacDonald, and P. G. Scherer, Biochemistry **26**, 7535 (1987).

[48] P. M. Macdonald and J. Seelig, Biochemistry **26**, 1231 (1987).

[49] H. Akutsu and J. Seelig, Biochemistry **20**, 7366 (1981).

[50] A. Catte, M. Girych, M. Javanainen, C. Loison, J. Melcr, M. S. Miettinen, L. Monticelli, J. Maatta, V. S. Oganesyan, O. H. S. Ollila, et al., Phys. Chem. Chem. Phys. **18**, 32560 (2016).

[51] J. Melcr, H. Martinez-Seara, R. Nencini, J. Kolafa, P. Jungwirth, and O. H. S. Ollila, The Journal of Physical Chemistry B **122**, 4546 (2018).

[52] J. Melcr, T. M. Ferreira, P. Jungwirth, and O. H. S. Ollila, Journal of Chemical Theory and Computation **16**, 738 (2020).

ToDo